Chemistry in Molten Alkali Metal Polyselenophosphate Fluxes. Influence of Flux Composition on Dimensionality. Layers and Chains in $APbPSe_4$, $A_4Pb(PSe_4)_2$ (A = Rb, Cs), and $K_4Eu(PSe_4)_2$

Konstantinos Chondroudis, Timothy J. McCarthy, and Mercouri G. Kanatzidis*

Department of Chemistry, Michigan State University, East Lansing, Michigan 48824

Received April 20, 1995[⊗]

The reaction of Pb and Eu with a molten mixture of $A_2Se/P_2Se_5/Se$ produced the quaternary compounds $APbPSe_4$, $A_4Pb(PSe_4)_2$ (A = Rb,Cs), and $K_4Eu(PSe_4)_2$. The red crystals of $APbPSe_4$ are stable in air and water. The orange crystals of $A_4Pb(PSe_4)_2$ and $K_4Eu(PSe_4)_2$ disintegrate in water and over a long exposure to air. $CsPbPSe_4$ crystallizes in the orthorhombic space group *Pnma* (No. 62) with $a = 18.607(4)$ Å, $b = 7.096(4)$ Å, $c = 6.612(4)$ Å, and $Z = 4$. $Rb_4Pb(PSe_4)_2$ crystallizes in the orthorhombic space group *Ibam* (No. 72) with $a = 19.134(9)$ Å, $b = 9.369(3)$ Å, $c = 10.488(3)$ Å, and $Z = 4$. The isomorphous $K_4Eu(PSe_4)_2$ has $a = 19.020(4)$ Å, $b = 9.131(1)$ Å, $c = 10.198(2)$ Å, and $Z = 4$. The $APbPSe_4$ have a layered structure with $[PbPSe_4]_n^{n-}$ layers separated by A^+ ions. The coordination geometry around Pb is trigonal prismatic. The layers are composed of chains of edge sharing trigonal prisms running along the *b*-direction. $[PSe_4]^{3-}$ tetrahedra link these chains along the *c*-direction by sharing edges and corners with the trigonal prisms. $A_4M(PSe_4)_2$ (M = Pb, Eu) has an one-dimensional structure in which $[M(PSe_4)_2]_n^{n-}$ chains are separated by A^+ ions. The coordination geometry around M is a distorted dodecahedron. Two $[PSe_4]^{3-}$ ligands bridge two adjacent metal atoms, using three selenium atoms each, forming in this way a chain along the *c*-direction. The solid state optical absorption spectra of the compounds are reported. All compounds melt congruently in the 597−620 °C region.

Introduction

Recently, we suggested the use of polychalcophosphate fluxes as an important foundation for exploratory synthesis of ternary and quaternary thiophosphate and selenophosphate complexes. These fluxes are formed by simple *in situ* fusion of $A_2Q/P_2Q_5/Q$.[1−3] The melts contain both polychalcogenide species and $[P_yQ_z]^{n-}$ ligands (Q = S, Se), and in this context, they become more like a bona fide solvent in which the coordination chemistry of chalcophosphates can be explored. Therefore, it becomes conceptually possible to form any such ligand *in situ* with the only limitation being that they have the modest (in solid state terms) thermal stability necessary to remain viable within the flux. We have shown that novel solid state structures can be constructed from $[P_2S_7]^{4-}$, $[PS_4]^{3-}$, and $[P_2Se_6]^{4-}$.[1−3] The first compound reported from a $A_xP_yS_z$ flux reaction at intermediate temperature was $ABiP_2S_7$ (A = K, Rb).[1] The selenide containing fluxes gave rise to several novel compounds such as $A_2MP_2Se_6$,[2,4] KMP_2Se_6 (M = Sb, Bi),[3] and $Cs_8M_4(P_2Se_6)_5$ (M = Sb,Bi),[2] with the latter two featuring astonishingly complex structures. Investigation of the lead system in such fluxes seems particularly interesting because the two known compounds $Pb_2P_2S_6$[5] and $Pb_2P_2Se_6$[5] as well as their Sn-analogs display interesting ferroelectric properties and phase transitions.[6] Furthermore, it appears that only a few Pb/P/Q ternary phases are known while no quaternary phase exists. Given that some lanthanides exhibit in many cases similar coordination to Pb^{2+} and can substitute this ion in the lattice we also made parallel investigations in the Eu system. Here we report the synthesis, structural characterization, optical and thermal properties of five new quaternary compounds, namely, $APbPSe_4$, $A_4Pb(PSe_4)_2$ (A = Rb, Cs), and $K_4Eu(PSe_4)_2$. Structural studies have been done for $CsPbPSe_4$, $Rb_4Pb(PSe_4)_2$, and $K_4Eu(PSe_4)_2$ while $RbPbPSe_4$ and $Cs_4Pb(PSe_4)_2$ proved to be X-ray isomorphous. All compounds feature novel structures containing the rare $[PSe_4]^{3-}$. To the best of our knowledge this unit exists in only a handful of compounds, including Cu_3PSe_4,[7] Tl_3PSe_4,[8] and the molecular $[WSe(PSe_2)(PSe_4)]^{2-}$.[9] In most selenophosphate compounds it is the ethane-like $[P_2Se_6]^{4-}$ unit that occurs as a structural building block.

Experimental Section

Reagents. The reagents mentioned in this study were used as obtained unless noted otherwise.

Syntheses. Compounds $APbPSe_4$ (A = Rb, Cs) were synthesized from a mixture of Pb (0.5 mmol), P (0.5 mmol), A_2Se (0.25 mmol), and Se (1.75 mmol) that was sealed under vacuum in a Pyrex tube and heated to 500 °C for 4 d followed by cooling to 150 °C at 4 °C h^{-1}. The products were washed with H_2O to reveal analytically pure dark red microcrystalline $APbPSe_4$ (85% yield based on Pb). The crystals are air- and water-stable. Single crystals were synthesized from a mixture of Pb (0.15 mmol), P_2Se_5 (0.30 mmol), A_2Se (0.30 mmol), and Se (1.5 mmol) that was sealed under vacuum in a Pyrex tube and heated to 450 °C for 4 d followed by cooling to 150 °C at 4 °C h^{-1}. The excess $A_xP_ySe_z$ flux was removed with DMF.

Compounds $A_4Pb(PSe_4)_2$ and $K_4Eu(PSe_4)_2$ were synthesized similarly from a mixture of Pb or Eu(0.15 mmol), P_2Se_5 (0.225 mmol), A_2Se (0.60), and Se (1.5 mmol) with the same heating conditions. The crystals of all three compounds are orange. They disintegrate in water

[⊗] Abstract published in *Advance ACS Abstracts,* January 1, 1996.

(1) McCarthy, T. J.; Kanatzidis, M. G. *Chem. Mater.* **1993**, *5*, 1061.
(2) McCarthy, T. J.; Hogan, T.; Kannewurf, C. R.; Kanatzidis, M. G. *Chem. Mater.* **1994**, *6*, 1072.
(3) McCarthy, T. J.; Kanatzidis, M. G. *J. Chem. Soc., Chem. Commun.* **1994**, 1089.
(4) McCarthy, T. J.; Kanatzidis, M. G. *Inorg. Chem.* **1995**, *34*, 1257.
(5) (a) Carpentier, C. D.; Nitsche, R. *Mater. Res. Bull.* **1974**, *9*, 1097. (b) Yun, H.; Ibers, J. A. *Acta Crystallogr.* **1987**, *C43*, 2002.
(6) Scott, B.; Pressprich, M.; Willet, R. D.; Clearly, D. A. *J. Solid State Chem.* **1992**, *96*, 294.
(7) Garin, J.; Parthe, E. *Acta Crystallogr.* **1972**, *B28*, 3672.
(8) Fritz, I. J.; Isaacs, T. J.; Gottlieb, M.; Morosin, B. *Solid State Commun.* **1978**, *29*, 535.
(9) O'Neal, S. C. O.; Pennington, W. T.; Kolis, J. W. *Angew. Chem., Int. Ed. Engl.* **1990**, *29*, 1486−1488.

0020-1669/96/1335-0840$12.00/0

and over a long exposure to air. In all cases yields were high, varying from 80% to 90% depending on the particular compound. Microprobe analysis with a scanning electron microscope (SEM), performed on a large number of single crystals, gave an average composition of $Cs_{0.8}PbPSe_{4.1}$ and $Rb_{3.8}PbP_2Se_{7.7}$.

Physical Measurements. Powder X-ray Diffraction. Analyses were performed using a calibrated Rigaku Rotaflex rotating anode powder diffractometer controlled by an IBM computer and operating at 45 kV/100 mA, employing Ni-filtered Cu radiation. Samples were ground to a fine powder and mounted by spreading the sample onto a piece of double-sided Scotch-brand tape affixed to a glass slide. For air sensitive compounds, samples were prepared in an N_2-filled glovebox and coated with mineral oil before analysis. Powder patterns were calculated with the CERIUS molecular modeling program by Molecular Simulations Inc., St. John's Innovation Centre, Cambridge, England.

Infrared Spectroscopy. Infrared spectra, in the region (600−50 cm^{-1}), were recorded on a computer-controlled Nicolet-740 Fourier Transform infrared spectrophotometer in 4 cm^{-1} resolution. Analyses were performed on finely ground solid samples using CsI as the pressed pellet matrix. For air sensitive compounds, samples were prepared in an N_2 filled glovebox and pressed into a pellet immediately upon removal.

Solid State UV/Vis/Near-IR Spectroscopy. Optical diffuse reflectance measurements were performed at room temperature using a Shimadzu UV-3101PC double beam, double monochromator spectrophotometer. The instrument is equipped with integrating sphere and controlled by a personal computer. $BaSO_4$ was used as a 100% reflectance standard for all materials. Samples are prepared by grinding them to a fine powder and spreading them on a compacted surface of the powdered standard material, preloaded into a sample holder. The reflectance vs wavelength data generated can be used to estimate a material's band gap by converting reflectance to absorption data as described earlier.[4]

Differential Thermal Analysis (DTA). DTA experiments were performed on a computer-controlled Shimadzu DTA-50 thermal analyzer. Typically a sample (∼15 mg) of ground crystalline material was sealed in quartz ampules under vacuum. A quartz ampule of equal mass filled with Al_2O_3 was sealed and placed on the reference side of the detector. The sample was heated to the desired temperature at 10 °C/min, then isothermed for 10 min, and finally cooled down to 100 °C at the same rate. Residue of the DTA experiment was examined by X-ray powder diffraction. To evaluate congruent melting we compared the X-ray powder diffraction patterns before and after the DTA experiments, as well as monitored the stability/reproducibility of the DTA diagrams upon cycling the above conditions at least two times.

Crystallography. Single-Crystal X-ray Diffraction. Intensity data was collected using a Rigaku AFC6S four-circle automated diffractometer equipped with a graphite crystal monochromator. An $\omega-2\theta$ scan mode was used. Crystal stability was monitored with three standard reflections whose intensities were checked every 150 reflections, and unless noted, no crystal decay was detected in any of the compounds. An empirical absorption correction based on ψ scans was applied to all data during initial stages of refinement. An empirical DIFABS correction[10] was applied after full isotropic refinement, after which full anisotropic refinement was performed. The structures were solved by direct methods using SHELXS-86 software[11a] (for all compounds), and full-matrix least-squares refinement was performed using the TEXSAN software package.[11b] All structures were solved by methods and software described elsewhere.[4] For $CsPbPSe_4$ data collected were 942 with 942 unique at $2\theta_{max} = 50°$. Data with $F_o^2 > 3\sigma(F_o^2)$ were 583. For $Rb_4Pb(PSe_4)_2$ total data collected were 968 with 968 unique at $2\theta_{max} = 50°$. Data with $F_o^2 > 3\sigma(F_o^2)$ were 560. For $K_4Eu(PSe_4)_2$ total data collected were 906 with 906 unique at $2\theta_{max} = 50°$. Data with $F_o^2 > 3\sigma(F_o^2)$ were 665. Crystallographic information for the compounds in this section are given in Table 1. The coordinates of all atoms, average temperature factors, and their estimated standard deviations are given in Tables 2−4.

(10) Walker, N.; Stuart, D. *Acta Crystallogr.* **1983**, *A39*, 158.
(11) (a) Sheldrick, G. M. In *Crystallographic Computing 3*; Sheldrick, G. M., Kruger, C., Doddard, R., Eds.; Oxford University Press: Oxford, England, 1985; p 175. (b) Gilmore, G. J. *Appl. Crystallogr.* **1984**, *17*, 42−46.

Table 1. Crystallographic Data for $CsPbPSe_4$, $Rb_4Pb(PSe_4)_2$, and $K_4Eu(PSe_4)_2$

	$CsPbPSe_4$	$Rb_4Pb(PSe_4)_2$	$K_4Eu(PSe_4)_2$
fw	686.92	1242.70	1001.98
a, Å	18.607(4)	19.134(9)	19.020(4)
b, Å	7.096	9.369(3)	9.131(1)
c, Å	6.612(4)	10.488(3)	10.198(2)
α, deg	90.0	90.0	90.0
β, deg	90.0	90.0	90.0
γ, deg	90.0	90.0	90.0
V, Å^3	873(1)	1880(2)	1771(1)
Z	4	4	4
λ(Mo Kα), Å	0.710 69	0.710 69	0.710 69
space group	*Pnma* (No. 62)	*Ibam* (No. 72)	*Ibam* (No. 72)
temp, °C	23	23	−100
ρ_{calc}, g/cm^3	5.226	4.390	3.757
μ, cm^{-1}	401.67	345.40	209.19
R^a, %	7.1	6.7	4.1
R_w,[a] %	8.0	8.1	5.2

[a] $R = \sum(|F_o| - |F_c|)/\sum|F_o|$. $R_w = \{\sum w(|F_o| - |F_c|)^2/\sum w|F_o|^2\}^{1/2}$.

Table 2. Positional Parameters and *B*(eq) for $CsPbPSe_4$

atom	*x*	*y*	*z*	*B*(eq)[a]
Pb	0.4819(1)	1/4	0.2905(3)	3.4(1)
Cs	0.7076(2)	1/4	−0.0513(6)	3.5(2)
Se(1)	0.3409(2)	1/4	0.0575(6)	1.9(2)
Se(2)	0.6177(2)	0.4992(4)	0.4028(4)	2.0(1)
Se(3)	0.5210(3)	1/4	−0.1496(7)	3.7(2)
P	0.4050(4)	1/4	−0.220(2)	0.9(4)

[a] $B_{eq} = (4/3)[a^2B(1,1) + b^2B(2,2) + c^2B(3,3) + ab(\cos\gamma)B(1,2) + ac(\cos\beta)B(1,3) + bc(\cos\alpha)B(2,3)$.

Table 3. Positional Parameters and *B*(eq) for $Rb_4Pb(PSe_4)_2$

atom	*x*	*y*	*z*	*B*(eq)[a]
Pb(1)	0	0	1/4	2.1(1)
Rb(1)	0.0872(3)	0.3813(5)	0	1.9(2)
Rb(2)	0.2371(3)	0	1/4	3.1(2)
Se(1)	0.0764(2)	0.2927(3)	0.3298(3)	1.8(2)
Se(2)	0.1054(2)	0.0287(4)	0	2.0(2)
Se(3)	0.2628(2)	0.2447(5)	0	1.6(2)
P(1)	0.1260(5)	0.203(1)	1/2	0.4(4)

[a] $B_{eq} = (4/3)[a^2B(1,1) + b^2B(2,2) + c^2B(3,3) + ab(\cos\gamma)B(1,2) + ac(\cos\beta)B(1,3) + bc(\cos\alpha)B(2,3)$.

Table 4. Positional Parameters and *B*(eq) for $K_4Eu(PSe_4)_2$

atom	*x*	*y*	*z*	*B*(eq)[a]
Eu	0	0	1/4	0.93(5)
Se(1)	0.07802(7)	0.3010(1)	0.3267(1)	1.42(5)
Se(2)	0.1052(1)	0.0319(2)	0	1.08(7)
Se(3)	0.2583(1)	0.2473(2)	0	1.42(8)
P(1)	0.1286(2)	0.2056(5)	1/2	0.8(2)
K(1)	0.0847(2)	0.3827(4)	0	1.7(2)
K(2)	0.2405(2)	0	1/4	2.2(2)

[a] $B_{eq} = (4/3)[a^2B(1,1) + b^2B(2,2) + c^2B(3,3) + ab(\cos\gamma)B(1,2) + ac(\cos\beta)B(1,3) + bc(\cos\alpha)B(2,3)$.

Results and Discussion

$CsPbPSe_4$ has the two-dimensional layered structure shown in Figure 1. The $[PbPSe_4]_n^{n-}$ layers are separated by Cs^+ ions which have an irregular seven coordination [Cs−Se mean = 3.7(1) Å]. The layers are composed of $PbSe_6$ trigonal prisms and $[PSe_4]^{3-}$ tetrahedra, as illustrated in Figure 2A. The atom connectivity within a single layer is more clearly viewed in Figure 2B. The trigonal prisms share rectangular edges in such

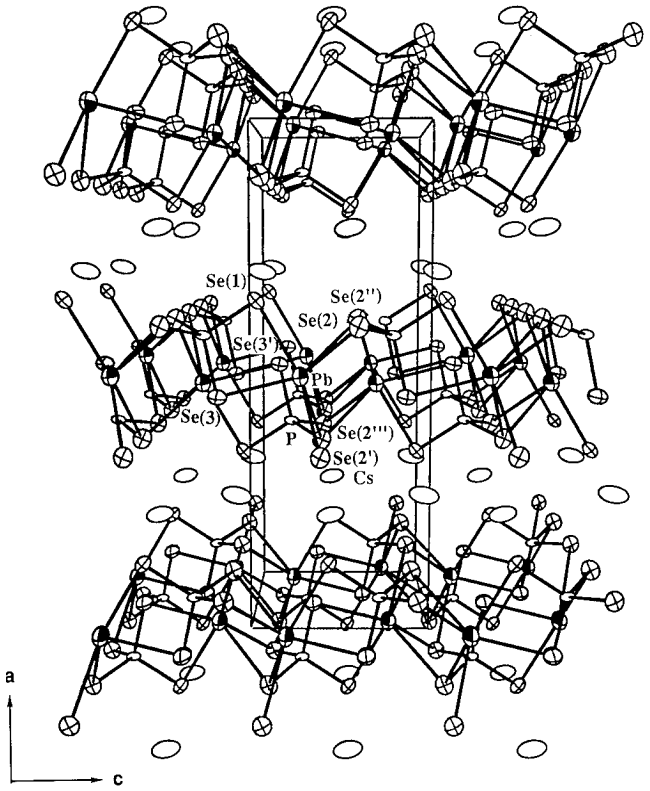

Figure 1. Extended structure of $CsPbPSe_4$ looking down the *b*-axis.

a way that the trigonal faces of the prisms point alternatively up and down forming parallel chains along the *b*-axis. These chains are then joined by $[PSe_4]^{3-}$ tetrahedra by sharing edges with the rectangles of the trigonal prisms; see polyhedral representation Figure 2A. The closest related compound is the ternary $Pb_2P_2Se_6$, but the two structures are fundamentally different. The more common $[P_2Se_6]^{4-}$ unit is present instead of the $[PSe_4]^{3-}$ in $CsPbPSe_4$, and the distorted bicapped trigonal prismatic coordination of Se atoms about the Pb atom in $Pb_2P_2Se_6$ is different from the trigonal prismatic arrangement in $CsPbPSe_4$. The Pb−Se distances in the latter range from 3.000(5) to 3.273(4) Å and compare very well with those found in $Pb_2P_2Se_6$[5] [3.096(2)−3.302(2) Å]. The P−Se distances range from 2.191(7) to 2.21(1) Å, the shortest being the one not bonded to Pb^{2+}. These distances are similar to those found in $[WSe(PSe_2)(PSe_4)]^{2-}$.[9] Similar distances have also been observed in $Pb_2P_2Se_6$,[5] $Hg_2P_2Se_6$,[12] and KMP_2Se_6 (M = Sb, Bi).[3] Tables of selected distances and angles for $CsPbPSe_4$ are given in Table 5.

The $Rb_4Pb(PSe_4)_2$ and its europium analog, $K_4Eu(PSe_4)_2$, have the same one-dimensional structure shown in Figure 3. Therefore, only the Pb compound will be discussed in detail. Every lead atom coordinates to four $[PSe_4]^{3-}$ units and becomes eight-coordinate, giving rise to an unusual coordination geometry of a distorted dodecahedron; see Figure 4. This type of coordination dodecahedron with its idealized D_2 symmetry is relatively rare. It has only triangular faces with no more than three selenium atoms lying strictly in a single plane. Two $[PSe_4]^{3-}$ ligands bridge two adjacent lead atoms in the chain employing three selenium atoms each. The fourth Se atom remains nonbonding. The Pb−Se distances range from 3.218(3) to 3.319(3) Å and compare very well with those mentioned above. The P−Se distances range from 2.188(7) to 2.21(1) Å, in good agreement with those of $CsPbPSe_4$. The $Pb_2P_2Se_6$ is the closest relative to this compound, but there are no structural similarities. There are two crystallographically independent Rb^+ ions, one having an eight-coordinate environment [Rb(1)−Se

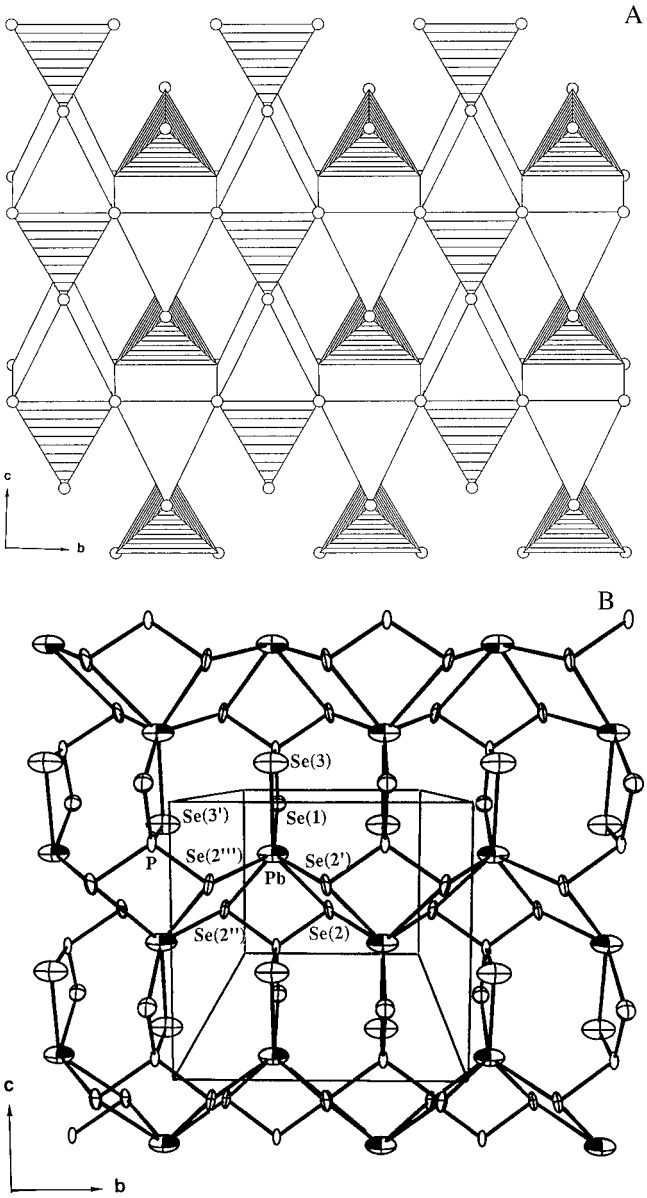

Figure 2. (A) Polyhedral representation of $CsPbPSe_4$ looking down the *a*-axis. (B) Structure and labeling of one layer of $CsPbPSe_4$ looking down the *a*-axis.

Table 5. Intramolecular Distances (Å) and Angles (deg) for $CsPbPSe_4$

Pb−Se(1)	3.042(4)	Se(1)−P	2.19(1)
Pb−Se(2)	3.273(4)	Se(3)−P	2.21(1)
Pb−Se(2′)	3.173(4)	Se(2)−P	2.191(7)
Pb−Se(3)	3.000(5)		
Cs−Se(1)	3.661(2)	Cs−Se(2′)	3.865(5)
Cs−Se(2)	3.719(4)	Cs−Se(3)	3.533(6)
Se(1)−Pb−Se(2)	143.65(7)	Se(1)−P−Se(2‴)	110.9(3)
Se(1)−Pb−Se(2′)	80.0(1)	Se(1)−P−Se(3′)	110.8(5)
Se(1)−Pb−Se(3)	73.6(1)	Se(2″)−P−Se(2‴)	108.6(5)
Se(2)−Pb−Se(2″)	67.8(1)	Se(2‴)−P−Se(3′)	107.7(3)
Se(2)−Pb−Se(2‴)	127.50(7)		
Se(2)−Pb−Se(2′)	90.15(9)	Se(2)−Se(2′)−Se(2‴)	90.14(7)
Se(2′)−Pb−Se(3)	91.9(1)	Se(2‴)−Se(2″)−Se(2)	89.86(7)
Se(2′)−Pb−Se(2‴)	65.9(1)	Se(2)−Se(1)−Se(2″)	52.0(1)
Se(2)−Pb−Se(3)	137.61(9)	Se(1)−Se(2″)−Se(2)	64.02(5)
Pb−Se(2)−Pb	89.85(9)	Se(2′)−Se(3)−Se(2‴)	46.95(9)
		Se(3)−Se(2‴)−Se(2′)	66.52(5)

(12) Jandali, M. Z.; Eulenberger, G.; Hahn, H. *Z. Anorg. Allg. Chem.* **1978**, *447*, 105.

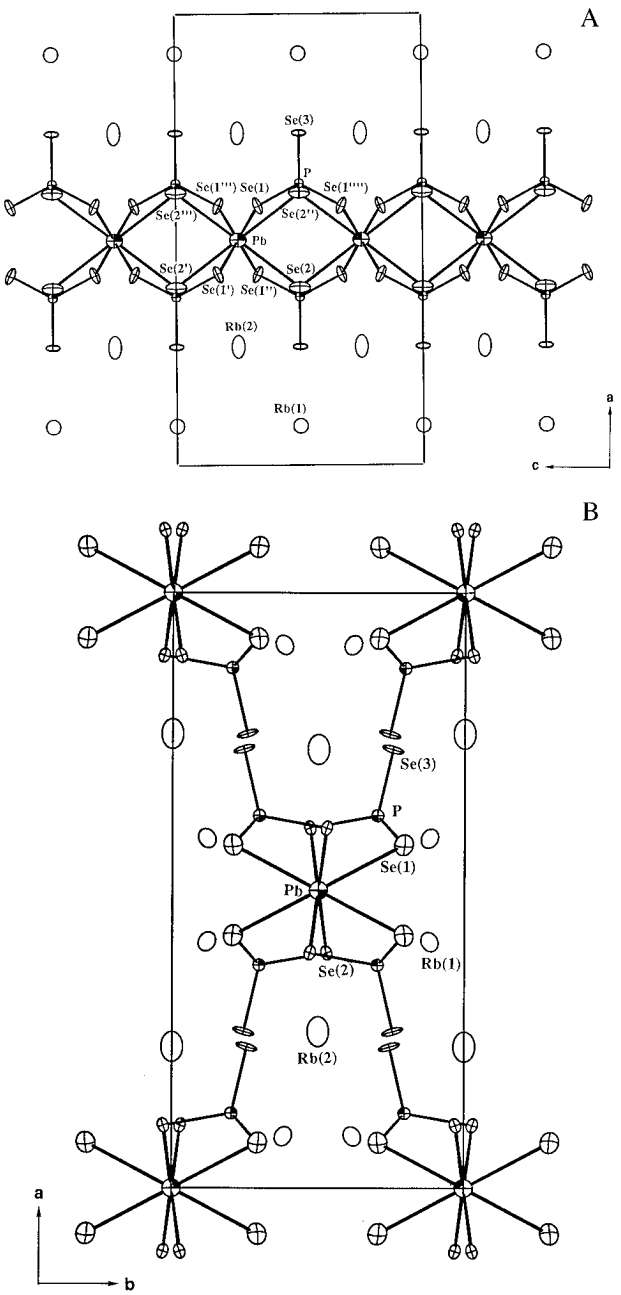

Figure 3. (A) Structure and labeling of one chain in $Rb_4Pb(PSe_4)_2$ looking down the *b*-axis. (B) Same structure looking down the *c*-axis.

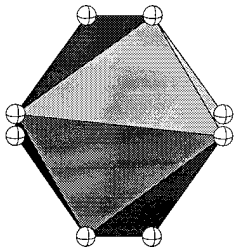

Figure 4. Coordination polyhedron of Pb in $Rb_4Pb(PSe_4)_2$.

mean 3.6(1) Å] with the other being six-coordinated [Rb(2)−Se mean 3.57(6) Å]. Comparison tables of selected distances and angles for the two isostructural compounds are given in Tables 6 and 7.

It is useful to consider the $APbPSe_4$ and $A_4Pb(PSe_4)_2$ as members of a series of compounds of the type $(A_3PSe_4)_n[Pb_3(PSe_4)_2]_m$ where $n = 1$, $m = 1$ and where $n = 4$, $m = 1$ respectively. $Pb_3(PSe_4)_2$ is the parent member ($n = 0$, $m = 1$) of the series. This compound is not known but its sulfur analog is[13] and has a three-dimensional structure. One can envision dismantling the 3-D network of $Pb_3(PSe_4)_2$ by introducing $[PSe_4]^{3-}$ units in its structure to obtain the 2-D network of $APbPSe_4$. Additional introduction of $[PSe_4]^{3-}$ results in the 1-D chains of the $A_4Pb(PSe_4)_2$ phase. To maintain electroneutrality, of course, for every $[PSe_4]^{3-}$ unit that is introduced, three A^+ cations should follow. This is illustrated in Scheme 1.

Table 6. Intramolecular Distances (Å) in $Rb_4Pb(PSe_4)_2$ and $K_4Eu(PSe_4)_2$ with Estimated Standard Deviations

$Rb_4Pb(PSe_4)_2$		$K_4Eu(PSe_4)_2$	
Pb−Se(1)	3.219(3)	Eu−Se(1)	3.220(1)
Pb−Se(2)	3.318(3)	Eu−Se(2)	3.254(1)
Rb(1)−Se(1)	3.698(6)	K(1)−Se(1)	3.641(4)
Rb(1)−Se(1′)	3.544(6)	K(1)−Se(1′)	3.388(3)
Rb(1)−Se(1″)	3.564(4)	K(1)−Se(1″)	3.417(2)
Rb(1)−Se(2)	3.322(6)	K(1)−Se(2)	3.227(4)
Rb(1)−Se(3)	3.596(7)	K(1)−Se(3)	3.527(5)
Rb(2)−Se(2″)	3.648(5)	K(2)−Se(2″)	3.635(4)
Rb(2)−Se(3)	3.517(3)	K(2)−Se(3)	3.423(1)
Rb(2)−Se(3′)	3.549(3)	K(2)−Se(3′)	3.439(1)
Se(1)−P	2.188(7)	Se(1)−P	2.193(3)
Se(2)−P	2.21(1)	Se(2)−P	2.214(5)
Se(3)−P	2.18(1)	Se(3)−P	2.194(5)

Table 7. Intramolecular Bond Angles (deg) for $Rb_4Pb(PSe_4)_2$ and $K_4Eu(PSe_4)_2$

$Rb_4Pb(PSe_4)_2$		$K_4Eu(PSe_4)_2$	
Se(1)−Pb−Se(1′)	63.1(1)	Se(1)−Eu−Se(1′)	62.79(5)
Se(1)−Pb−Se(1″)	149.8(1)	Se(1)−Eu−Se(1″)	151.89(4)
Se(1)−Pb−Se(1‴)	126.0(1)	Se(1)−Eu−Se(1‴)	125.11(5)
Se(1)−Pb−Se(2)	90.08(9)	Se(1)−Eu−Se(2)	90.95(4)
Se(1)−Pb−Se(2′)	123.40(9)	Se(1)−Eu−Se(2′)	123.37(3)
Se(1)−Pb−Se(2″)	65.63(9)	Se(1)−Eu−Se(2″)	66.60(3)
Se(1)−Pb−Se(2‴)	81.99(9)	Se(1)−Eu−Se(2‴)	80.25(4)
Se(2)−Pb−Se(2′)	105.2(1)	Se(2)−Eu−Se(2′)	104.14(5)
Se(2)−Pb−Se(2″)	75.6(1)	Se(2)−Eu−Se(2″)	76.81(5)
Se(2)−Pb−Se(2‴)	170.7(1)	Se(2)−Eu−Se(2‴)	169.73(5)
Pb−Se(1)−P	94.7(3)	Eu−Se(1)−P	93.4(1)
Pb−Se(2)−P	91.7(2)	Eu−Se(2)−P	92.06(8)
Pb−Se(2)−Pb	104.4(1)	Eu−Se(2)−Eu	103.19(5)
Se(1)−P−Se(1⁗)	109.3(5)	Se(1)−P−Se(1⁗)	107.4(2)
Se(1)−P−Se(2″)	107.5(3)	Se(1)−P−Se(2″)	107.5(1)
Se(1)−P−Se(3)	109.6(3)	Se(1)−P−Se(3)	110.6(1)
Se(3)−P−Se(2″)	113.2(5)	Se(3)−P−Se(2″)	112.9(2)

Scheme 1

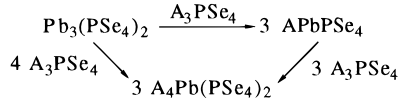

Access to each phase is achieved by modification of flux composition. Specifically, to obtain the $APbPSe_4$ phase, a ratio of 1:2:2:10 of $Pb/P_2Se_5/A_2Se/Se$ was used. Doubling the amount of A_2Se and thus increasing the basicity of the flux lead to the next member of the series, $A_4Pb(PSe_4)_2$. A possible next member of the composition $A_7Pb(PSe_4)_3$ cannot be ruled out but it is likely to be a molecular compound. The reaction conditions that lead to the parent $Pb_3(PSe_4)_2$ are under investigation.[14]

The solid-state UV/vis diffuse reflectance spectra of the compounds spectra reveal sharp optical gaps consistent with semiconductors. The $APbPSe_4$ (A = Rb, Cs) compounds show band gaps, E_g, of 2.07 and 2.08 eV, respectively (see Figure

(13) Post, E.; Kramer, V. *Mater. Res. Bull.* **1984**, *19*, 1607.
(14) Chondroudis, K.; Kanatzidis M. G. Work in progress.

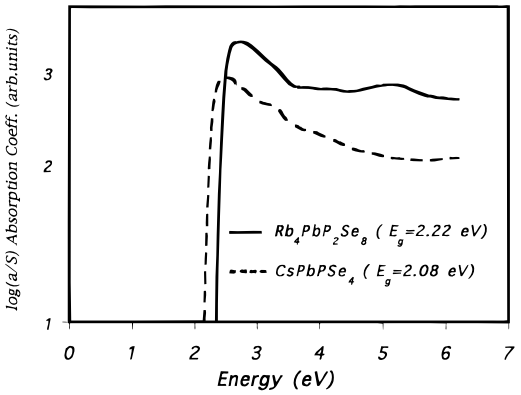

Figure 5. Solid-state optical absorption spectra of $CsPbPSe_4$ and $Rb_4Pb(PSe_4)_2$.

5), while $A_4Pb(PSe_4)_2$ show 2.22 and 2.26 eV, respectively. The larger energy gaps in the latter compounds are consistent with the lower dimensionality of their structure. The far-IR spectraof $APbPSe_4$ display two strong absorptions at ~433 and ~450 cm^{-1}. Accordingly, $A_4Pb(PSe_4)_2$ and $K_4Eu(PSe_4)_2$ display two strong absorptions at ~428 and ~440 cm^{-1}. These vibrations can be assigned to PSe_4 stretching modes and are of diagnostic value in distinguishing this selenophosphate ligand from others.[4] All compounds possess weak absorptions below 200 cm^{-1} which probably are due to Pb−Se vibrations.

Differential thermal analysis (DTA) data, see Figure 6, show that the compounds melt congruently. In particular, $RbPbPSe_4$ and $CsPbPSe_4$ melt at 597 and 612 °C, respectively, whereas $Rb_4Pb(PSe_4)_2$, $Cs_4Pb(PSe_4)_2$ and $K_4Eu(PSe_4)_2$ melt at 615, 616, and 620 °C, respectively.

In conclusion, the synthesis of these new members of the A/M/P/Se family emphasizes the usefulness of the polyselenophosphate $A_x[P_ySe_z]$ fluxes in the synthesis of complex new chalcophosphate compounds. In the case of Eu and Pb the fluxes provided a convenient entry into their little known quaternary chemistry and is expected to do the same in other systems.[15] Control of flux composition results in compounds with different compositions where the $[PSe_4]^{3-}$ ligand content can be adjusted to produce two-dimensional and one-dimensional structures. The overwhelming occurrence of the $[P_2Se_6]^{4-}$ unit vs the $[PSe_4]^{3-}$ in the compounds reported thus far in the literature suggest that the tetrahedral P^{5+} species is unstable with respect to the dimeric P^{4+} species under the conventional synthetic conditions employed. The $A_x[P_ySe_z]$ fluxes provide a novel and perhaps unique medium which is basic enough to stabilize the $[PSe_4]^{3-}$ unit and make it available for coordination.

(15) Chondroudis, K.; Kanatzidis M. G. To be submitted for publication.

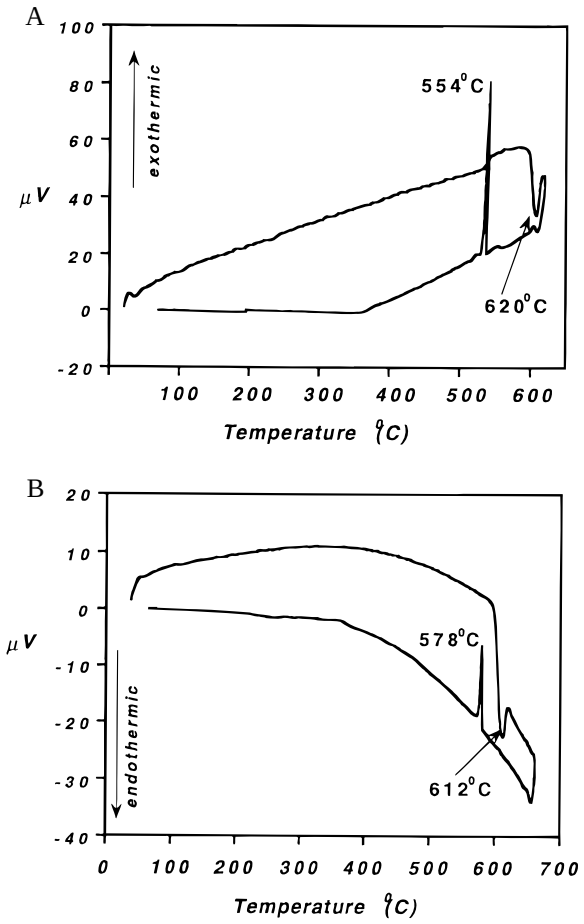

Figure 6. DTA diagrams for (A) $K_4Eu(PSe_4)_2$ and (B) $CsPbPSe_4$. The melting and crystallization events are indicated by the endothermic and exothermic peaks respectively. Heating rate: 10 deg/min.

Acknowledgment. Financial support from the National Science Foundation DMR-9202428 is gratefully acknowledged. M.G.K. is an A. P. Sloan Foundation and a Camille and Henry Dreyfus Teacher-Scholar 1993−1995. This work made use of the SEM facilities of the Center for Electron Optics at Michigan State University.

Note Added in Proof. While this paper was undergoing review, a publication reporting the synthesis of $KLaP_2Se_6$ from a polyselenophosphate flux appeared: Chen, J. H.; Dorhout, P. K. *Inorg. Chem.* **1995**, *34*, 5705−5706.

Supporting Information Available: Tables of crystallographic details, fractional atomic coordinates of all atoms, anisotropic and isotropic thermal parameters of all atoms, interatomic distances and angles, and calculated and observed X-ray powder patterns for $CsPbPSe_4$, $Rb_4Pb(PSe_4)_2$, and $K_4Eu(PSe_4)_2$ (34 pages). Ordering information is given on any current masthead page.

IC950479+